Eur. Phys. J. Plus (2021) 136:577
https://doi.org/10.1140/epjp/s13360-021-01593-8

THE EUROPEAN PHYSICAL JOURNAL PLUS

Regular Article

Changes in blood–brain barrier permeability characterized from electroencephalograms with a combined wavelet and fluctuation analysis

A. N. Pavlov[1,a], **A. P. Khorovodov**[1], **A. T. Mamedova**[1], **A. A. Koronovskii Jr.**[1], **O. N. Pavlova**[1], **O. V. Semyachkina-Glushkovskaya**[1], **J. Kurths**[1,2,3]

[1] Saratov State University, Astrakhanskaya 83, Saratov 410012, Russia
[2] Potsdam Institute for Climate Impact Research, Telegraphenberg A 31, Potsdam 14473, Germany
[3] Institute of Physics, Humboldt University Berlin, Berlin 12489, Germany

Received: 14 March 2021 / Accepted: 19 May 2021

Abstract We study changes in the blood–brain barrier (BBB) permeability in mice caused by a 2-h intermittent sound and discuss their reflection in the electrical activity of the brain. Using the detrended fluctuation analysis (DFA), multiresolution wavelet analysis (MWA) and their recent modifications, we compare the capabilities of reliably characterizing the transitions between closed and open BBB states. It is shown that an enhanced approach, combining MWA with DFA of the decomposition coefficients, improves the interstate separation by limiting the most appropriate level of resolution. This approach can be useful in various studies of complex systems based on experimental data.

1 Introduction

The blood–brain barrier (BBB) is an important protective element that is essential for our survival [1,2]. It contains tight junctions preventing the transfer of molecules between blood vessels and the brain. The BBB mainly consists of the endothelial cells of the brain capillaries, astroglia and pericytes. Its complex organization ensures semipermeability when blood-borne agents cannot pass through it, although glucose, water and amino acids overcome the BBB. On the one hand, preventing the passive diffusion of many types of molecules into the brain avoids the transport of circulating pathogens, and hence, this key homeostatic mechanism for the central nervous system maintains the health of the body. However, on the other hand, such a border does not allow the transport of drugs to the brain in the treatment of various injuries.

Early studies [3,4] showed that stressful conditions and, in particular, prolonged immobilization stress increase BBB permeability, although the underlying mechanisms were not fully understood [5]. Taking into account the role of the BBB, it has been suggested that such changes may contribute to impaired brain functions. Over the past decade, the possibility of opening the BBB due to external influences such as focused ultrasound, which is a noninvasive and nonionizing therapeutic method, has been proven and widely discussed [6–15].

[a] e-mail: pavlov.alexeyn@gmail.com (corresponding author)

Published online: 25 May 2021

A pioneering clinical study of ultrasound and microbubbles for the temporary opening of the BBB was described in [16]. Injection of microbubbles before the application of focused ultrasound makes it possible to concentrate the acoustic effect on the cerebral blood vessels.

It is important to note that increasing the BBB permeability is a reversible procedure, and the BBB returns to its normal (closed) state after a few hours. The latter allows for a relatively short period of time to carry out the necessary transport of drugs for therapeutic purposes until the normal function of the BBB is restored. A fairly safe way to open the BBB [17–19] is to use loud music or intermittent sound for 2 h. Its ability to increase the BBB permeability has been confirmed in laboratory animals using a number of experimental methods and histological analysis. In particular, it was found that the BBB opens up to 1 hour and closes from 1 to 4 h after sound exposure [17]. Thus, listening to loud music for 2 hours in an intermittent adaptive mode is accompanied by a delayed (1 h after music exposure) and short-lasting to (1–4 h) opening of the BBB to low- and high-molecular-weight compounds without cochlear and brain impairments [17].

Changes in the BBB permeability are reflected in the electrical signals of the brain, measured by electroencephalograms (EEG). Our previous study [20] showed how such changes are detected in terms of long-range power-law correlations. For this purpose, we compared the state of the BBB opening with the background electrical activity of the brain and found a decrease in the scaling exponents of the extended detrended fluctuation analysis (EDFA) [21,22]. Although the differences between the states were significant for the group of animals, the recordings were carried out under different conditions—before and after sound exposure (e.g., in different days). Hence, the reaction could be caused not only by sound, but also by stressful conditions. In contrast to the work [20], now we consider recordings made at one time (dynamics after 2 h of sound exposure), which allows us to reduce possible effects of different physiological conditions. We are also conducting a more detailed analysis of the experiments by combining different data processing tools. In addition to the detrended fluctuation analysis (DFA) [23–25], we apply multiresolution wavelet analysis (MWA) based on a discrete wavelet transform (DWT) [26–28] and our recently proposed approach, enhanced multiresolution wavelet analysis [29]. This way we combine a signal decomposition procedure with DFA of detail wavelet coefficients at different levels of resolution. In the course of a comparative analysis, we will demonstrate the significant potential of this combined tool for elaboration reliable markers of the BBB opening.

The manuscript is organized as follows. Section 2 describes the standard versions of DFA and MWA and the proposed approaches extending their performances. In addition, this section contains information about experiments on mice that increase the BBB permeability, and a description of the datasets acquired. Results showing the potential of the modified tools and their discussion are provided in Sect. 3. Section 4 summarizes the main findings.

2 Methods and experiments

2.1 DFA

Detrended fluctuation analysis [23–25] is a variant of the correlation analysis of complex processes, including nonstationary datasets, which is especially useful for studying long-range correlations. Its basic algorithm includes the transition from a signal $x(i), i = 1, \ldots, N$

to its profile $y(k)$

$$y(k) = \sum_{i=1}^{k} [x(i) - \langle x \rangle], \quad \langle x \rangle = \sum_{i=1}^{N} x(i), \quad k = 1, \ldots, N, \tag{1}$$

its segmentation into parts of length n ($n < N$), the estimation of the local trend $y_n(k)$ within each segment and the computation of the standard deviation of $y(k)$ from $y_n(k)$

$$F(n) = \sqrt{\frac{1}{N} \sum_{k=1}^{N} [y(k) - y_n(k)]^2}. \tag{2}$$

When such estimates are performed over a wide range of n, a possible power-law dependence

$$F(n) \sim n^{\alpha} \tag{3}$$

is analyzed, and the scaling exponent α is computed. The relation (3) is typical for stochastic processes, although the properties of short-range and long-range correlations may differ. DFA has become a useful approach in different research areas [30–33].

2.2 MWA

Multiresolution wavelet analysis [26–28] is another wide-spread method for processing non-stationary signals. It decomposes a signal $x(t) \in L^2(R)$ using two bases constructed from the scaling function $\varphi(t)$ and the wavelet $\psi(t)$

$$x(t) = \sum_{k} s_{j_n,k} \varphi_{j_n,k}(t) + \sum_{j \le j_n} \sum_{k} d_{j,k} \psi_{j,k}(t) \tag{4}$$

where j_n is the selected resolution level. The bases are composed by dilations and translations of $\varphi(t)$ and $\psi(t)$ and form two sets of conjugate mirror filters: low-pass and high-pass filters, respectively

$$\varphi_{j,k}(t) = 2^{-j/2} \varphi\left(2^{-j} t - k\right), \quad \psi_{j,k}(t) = 2^{-j/2} \psi\left(2^{-j} t - k\right). \tag{5}$$

MWA allows the use of a fast decomposition algorithm for integer values j and k. The transitions between resolution levels are performed according to the rules

$$\varphi(t) = \sqrt{2} \sum_{k=0}^{2M-1} h_k \varphi(2t - k), \quad \psi(t) = \sqrt{2} \sum_{k=0}^{2M-1} g_k \psi(2t - k), \tag{6}$$

where $2M$ is the number of filter coefficients, $g_k = (-1)^k h_{2M-k-1}$. The coefficients h_k and g_k are given *a priory* for each wavelet function, e.g., the Daubechies family [27]. The choice of an appropriate function depends on the aims of the research and is based on a trade-off between the regularity property (the number of vanishing moments) and the support length. In many practical cases, the D^8 Daubechies wavelet is used. MWA is performed as a repetitive procedure for different timescales [27]. The analysis of the variability of the signal $x(t)$ is often carried out using the available sets of $d_{j,k}$ coefficients called detail coefficients. An important measure of their fluctuations is the standard deviation, computed depending on j

$$\sigma(j) = \sqrt{\frac{1}{J} \sum_{k=0}^{J-1} \left[d_{j,k} - \langle d_{j,k} \rangle\right]^2}, \quad \langle d_{j,k} \rangle = \sum_{k=0}^{J-1} d_{j,k}, \tag{7}$$

where J is the number of $d_{j,k}$ at the resolution level j. Several studies (e.g., [28,34]) have reported promising diagnostic results using the measure (7).

2.3 Modified approaches

The standard DFA and MWA approaches have some limitations. The first method mainly deals with rather homogeneous datasets and does not account for different features of nonstationary behavior throughout the signal, when some segments provide stronger root-mean-square (RMS) fluctuations compared to other parts of data or nonstationarity in energy. The second method considers fairly simple statistical characteristics of the decomposition coefficients, namely the standard deviations. The latter limits information on the complex organization of datasets, and the use of more informative measures characterizing, e.g., the correlation features of detail coefficients can expand diagnostic capabilities of this tool. In our recent publications [21,29], we have proposed modifications to these methods. Here, we briefly describe the main ideas of extended DFA (EDFA) [20–22] and enhanced MWA, which is a combined MWA&DFA method [29].

2.3.1 EDFA

If the RMS fluctuations $F(n)$ of $y(k)$ from $y_n(k)$ described by Eq. (2) show strong variations between segments, it becomes useful to analyze the local values $F_{loc}(n)$, and each of them is estimated within one segment of length n. For this purpose, we proposed to consider the standard deviation of the local RMS fluctuations $\sigma(F_{loc}(n))$ as a measure of the inhomogeneity of the signal profile [35]. This measure also shows a power-law behavior with n, which is described by the scaling exponent β

$$\sigma(F_{loc}(n)) \sim n^{\beta}. \tag{8}$$

β does not match α and can even take negative values. Both of these exponents characterize different features of the complex organization of experimental signals. A more detailed description of EDFA and its features for several types of nonstationarity are given in [36].

2.3.2 MWA&DFA

The combined MWA&DFA approach includes a standard signal decomposition procedure using bases of scaling functions as well as wavelets (5) with an estimate of the detail coefficients $d_{j,k}$ at each available resolution level j. Instead of standard deviations (7), we suggested performing the DFA of these coefficients [29]. The latter allows one to quantitatively estimate the correlations of wavelet coefficients at different scales and, therefore, to obtain more information about the structure of experimental datasets. On each scale j, a random walk of detail coefficients is constructed

$$y_j(l) = \sum_{k=0}^{l-1} \left[d_{j,k} - \langle d_{j,k} \rangle \right], \quad l = 1, \ldots, J, \tag{9}$$

which is further divided into segments of length $n \ll J$, and the trend $z_j(l)$ is estimated by the least-squares method. The RMS fluctuations

$$F_j(n) = \sqrt{\frac{1}{J} \sum_{l=1}^{J} [y_j(l) - z_j(l)]^2} \sim n^{\alpha_j} \tag{10}$$

are computed over a wide range of n to obtain the scaling exponent α_j. Unlike the standard DFA, here we analyze the features of the power-law correlations of the wavelet coefficients associated with different levels of resolution. The combined MWA&DFA approach thus evaluates the sequence of α_j, which can provide a more informative characterization of complex processes than the standard MWA [29].

2.4 Subjects and experiments

Experiments were carried out on eight male C57BL/6 mice (20–25 g) in accordance with the Guide for the Care and Use of Laboratory Animals and protocols approved by the Local Bioethics Commission of the Saratov State University. Mice were housed in a light/dark environment with lights on from 8:00 to 20:00 and fed *ad libitum* with standard rodent food and water. Before the experimental recordings, a surgery was performed that included mounting a head plate, drilling small burrs and inserting EEG wire leads into the burrs on one side of the midline between the skull and the dura mater. Dental acrylic was applied to fix the EEG leads, and ibuprofen (15 mg/kg) was used in the water supply for 2–3 days before and at least 3 days after surgery to reduce postoperative pain. A 10-day recovery from surgery was ensured.

After this recovery, we applied the BBB opening method described in [37], which is based on the use of a loud sound (100 dB, 370 Hz) for 2 hours in accordance with the exposure algorithm: 1 min—sound, 1 min—pause. At the end of the sound exposure, two-channel EEG signals (Pinnacle Technology, Taiwan) were measured using silver electrodes located on both sides of the midline for 2 hours. The sampling rate was 2 kHz.

3 Results and Discussion

According to earlier studies [17–19,37], the "window" of BBB opening in laboratory animals due to 2-hour intermittent sound exposure or loud music has been established and confirmed by various experimental methods, including two-photon microscopy, magnetic resonance imaging (MRI), fluorescence analysis, spectrofluorimetric and confocal analysis. In addition to optical techniques, a confirmation was also carried out on the basis of histological analysis of the tissue and blood vessels of the brain. These results allow us to expect that increased BBB permeability occurs approximately one hour after the end of sound exposure. Although this value depends on the subject, we can expect differences in BBB permeability during the first and second hours when the sound is turned off, and we also expect these changes to be reflected in the EEG measurements. Figure 1 shows a typical example of the behavior of EDFA scaling exponents assessed for 10-min segments of EEG data. Both α and β exponents are decreasing, but β demonstrates stronger changes. Figure 1 illustrates that α and β take on different values, especially when comparing the initial (0–30 min) and last (90–120 min) parts of the dependencies. The dashed line at 60 min indicates the expected BBB open position. The behavior of $\alpha(t)$ and $\beta(t)$ suggests that there is a fairly smooth transition between the closed and open BBB regimes, when its permeability increases. In order not to take into account the time boundary between these states, which in many cases may be undefined, we will compare both states without a transient and exclude the records related to the time interval from 40 to 80 min. Therefore, we will estimate the average amounts associated with the closed BBB (0–40 min) and open BBB (80–120 min) and compare them across the entire group of animals to study statistically significant interstate differences.

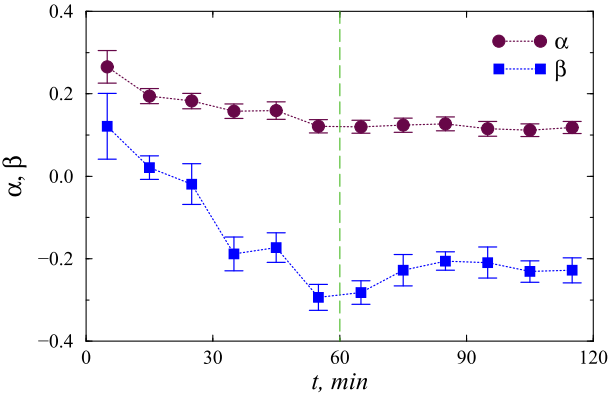

Fig. 1 A typical example of changes in the EDFA scaling exponents caused by 2-hour exposure of intermittent sound (mean values ± SE). Time is measured after the end of this procedure. The dashed line indicates the expected time of the BBB opening. Averaging is performed over different sets of algorithmic parameters

Let us consider the distinctions starting with EDFA. Our statistical analysis confirms the downward trend in both scaling exponents. The α exponent decreases by 0.08±0.03, significantly (Mann–Whitney test, $p<0.05$) for 5 out of 8 mice. In the rest of the animals, the changes in the values of α are rather small and are comparable with statistical errors. There were no animals showing a significant increase in the exponent quantifying long-range power-law correlations. The β exponent decreases by 0.19±0.07, i.e., it shows stronger changes with significant (Mann–Whitney test, $p<0.05$) interstate differences for 6 out of 8 mice (including 5 detected with the α exponent). Again, there were no animals demonstrating the opposite reaction. These results confirm the possibility of detecting the transition between closed and open BBB based on EEG signals, the measurement of which is rather simple compared to approaches such as MRI.

MWA based on standard deviations of detail coefficients provides separation of the states under study using $\sigma(j)$ dependencies. An example given in Fig. 2 illustrates the distinctions between the EEG signals recorded during the first and second hours after the end of the sound exposure. Similar to the EDFA scaling exponents, the variability of the detail coefficients also decreases with higher BBB permeability. In Fig. 2, we show the results for each 10-min segment of an EEG recording from one channel. A good interstate separation is observed, although the results for one segment do not match the overall behavior (circles in the middle of the σ-values associated with the closed BBB state). This means the absence of a clearly defined boundary between these states and the variability of EEG characteristics during the transient process. By analogy with the previous approach, it seems useful to exclude the segments related to the time interval from 40 to 80 minutes. In the latter case, a more reliable separation between states becomes possible, and we need to choose a resolution level at which the distinctions are well expressed. According to Fig. 2 and a preliminary analysis of other experimental data, the $j = 8$ scale is best suited for these purposes. The $\sigma(8)$ measure decreases from 403±10 to 354±4, showing significant distinctions (Mann–Whitney test, $p < 0.05$) for the same 6 out of 8 mice, i.e., the results are comparable to the EDFA approach. Similar results can be obtained for neighboring scales ($j = 7$ or $j = 9$), but a consideration of smaller j levels worsens the diagnostics.

The enhanced approach (MWA&DFA) dealing with a correlation analysis of detail coefficients also shows the strongest distinctions for the resolution levels $j = 7, 8, 9$, with the

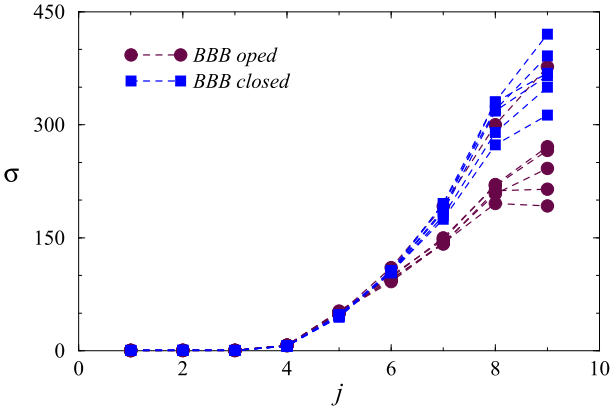

Fig. 2 Changes in the standard deviations of wavelet coefficients of the MWA method produced by the sound exposure (a typical example). Different curves are obtained for different 10-minute segments

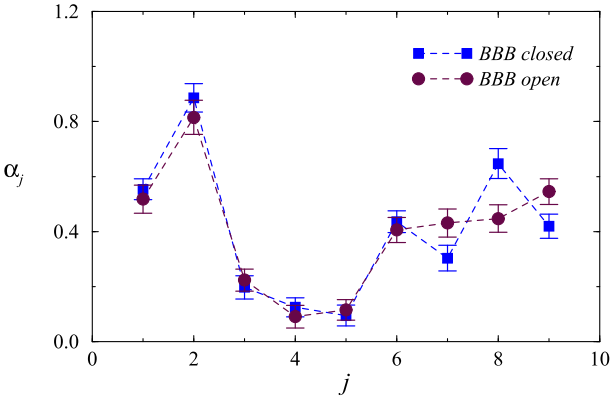

Fig. 3 An example of changes in the scaling exponents α_j of the MWA&DFA method produced by the sound exposure (mean values ± SD)

strongest response for $j = 8$ (Fig. 3). For better visualization of the observed distinctions, we give in Fig. 3 an example of sound-induced changes by averaging the results for the closed BBB (0–40 min) and open BBB (80–120 min) states. The behavior of α_j usually does not coincide with $\sigma(j)$, and a variability of correlation features for individual segments of EEG recordings can be observed for both simulated and experimental data sets [29]. Typically, a reduction of α_j appears when the BBB's permeability grows. In our study, this effect was observed in 7 out of 8 mice at the resolution level $j = 8$. The average values of α_8 decrease from 0.47±0.01 to 0.42±0.01. Thus, the latter approach provided the best interstate separation, although the results of all methods are comparable, and all of them can be applied to reveal the BBB opening. Unlike DFA-based techniques applied to EEG data, now we deal with pre-filtered sets of wavelet coefficients that are not distorted by components associated with inappropriate frequency ranges for diagnostics.

4 Conclusion

The semipermeability of the BBB is critical to prevent the transfer of circulating pathogens to the brain. However, this homeostatic mechanism interferes with the treatment of brain injuries when drug delivery to the brain is required. The topic of the short-term opening of the BBB for therapeutic purposes has been actively discussed in recent years, and rather safe noninvasive methods for increasing the BBB permeability have been proposed and verified. One of them, which is used in this study, consists of a 2-hour exposure of intermittent sound, leading to a short-term opening of the BBB about 1 hour after the end of this procedure.

In this study, we compare the potential of two standard methods, DFA and MWA, in detecting structural changes in EEG signals associated with changes in BBB permeability. We also consider recent modifications of these tools, namely the extended DFA (EDFA), which introduces an additional measure to characterize the features of nonstationary behavior throughout the signal, especially in cases of transients and nonstationarity in energy, as well as the enhanced MWA, which provides a correlation analysis of the detail decomposition coefficients unlike the simpler approach dealing with their standard deviations. The obtained results show that all these tools are helpful for diagnosing changes in BBB permeability. However, the latter approach, the combined MWA&DFA, provides a better separation between the states. These results can be explained by the choice of the appropriate level of resolution, when other components that are not essential for distinguishing between the closed and open BBB states are excluded and do not affect the assessment of diagnostic measures. Thus, a preliminary selection of the decomposition coefficients is provided for a better detection of transitions from the normal BBB function to its short-term opening. Hence, this is a fairly universal approach that can find a wide range of applications by improving the ability to extract information about the complex structure of experimental data in comparison with standard MWA.

Acknowledgements This work was supported by the RF Government grant No. 075-15-2019-1885. A.P. acknowledges support by the grant of the President of the Russian Federation for leading scientific schools (NSh-2594.2020.2).

References

1. N.J. Abbott, L. Rönnbäck, E. Hansson, Nat. Rev. Neurosci. **7**, 41 (2006)
2. W.M. Pardridge, Expert Opin. Drug Deliv. **13**, 963 (2016)
3. H.S. Sharma, P.K. Dey, Neurosci. Res. **5**, 224 (1988)
4. R. Cooper, Clin. Neurophysiol. **7**, B28 (1974)
5. C. Angel, Dis. Nerv. Syst. **30**, 94 (1969)
6. E.E. Konofagou, Y.S. Tung, J. Choi, T. Deffieux, B. Baseri, F. Vlachos, Curr. Pharm. Biotechnol. **13**, 1332 (2012)
7. M.E. Downs, A. Buch, C. Sierra, M.E. Karakatsani, T. Teichert, S. Chen, E.E. Konofagou, V.P. Ferrera, PLoS One **10**, e0125911 (2015)
8. S.Y. Wu, C. Aurup, C.S. Sanchez, J. Grondin, W. Zheng, H. Kamimura, V.P. Ferrera, E.E. Konofagou, Sci. Rep. **8**, 7978 (2018)
9. K.H. Song, B.K. Harvey, M.A. Borden, Theranostics **8**, 4393 (2018)
10. N. Lipsman, Y. Meng, A.J. Bethune, Y. Huang, B. Lam, M. Masellis, N. Herrmann, C. Heyn, I. Aubert, A. Boutet, G.S. Smith, K. Hynynen, S.E. Black, Nat. Commun. **9**, 2336 (2018)
11. Z. Deng, Z. Sheng, F. Yan, J. Oncol. **2019**, 2345203 (2019)
12. K.T. Chen, K.C. Wei, H.L. Liu, Front. Pharmacol. **10**, 86 (2019)
13. A.N. Pouliopoulos, S.Y. Wu, M.T. Burgess, M.E. Karakatsani, H.A.S. Kamimura, E.E. Konofagou, Ultrasound Med. Biol. **46**, 73 (2020)
14. K. Beccaria, M. Canney, G. Bouchoux, S. Puget, J. Grill, A. Carpentier, Neurosurg. Focus. **48**, E10 (2020)

15. C.T. Curley, B.P. Mead, K. Negron, N. Kim, W.J. Garrison, G.W. Miller, K.M. Kingsmore, E.A. Thim, J. Song, J.M. Munson, A.L. Klibanov, J.S. Suk, J. Hanes, R.J. Price, Sci Adv. **6**, eaay1344 (2020)
16. A. Carpentier, M. Canney, A. Vignot, V. Reina, K. Beccaria, C. Horodyckid, C. Karachi, D. Leclercq, C. Lafon, J.Y. Chapelon, L. Capelle, P. Cornu, M. Sanson, K. Hoang-Xuan, J.Y. Delattre, A. Idbaih, Sci. Transl. Med. **8**, 343re2 (2016)
17. O. Semyachkina-Glushkovskaya, A. Esmat, D. Bragin, O. Bragina, A.A. Shirokov, N. Navolokin, Y. Yang, A. Abdurashitov, A. Khorovodov, A. Terskov, M. Klimova, A. Mamedova, I. Fedosov, V. Tuchin, J. Kurths, Proc. Biol. Sci. **287**, 20202337 (2020)
18. O. Semyachkina-Glushkovskaya, D. Postnov, T. Penzel, J. Kurths, Int. J. Mol. Sci. **21**, 6293 (2020)
19. O. Semyachkina-Glushkovskaya, V. Chehonin, E. Borisova, I. Fedosov, A. Namykin, A. Abdurashitov, A. Shirokov, B. Khlebtsov, Y. Lyubun, N. Navolokin, M. Ulanova, N. Shushunova, A. Khorovodov, I. Agranovich, A. Bodrova, M. Sagatova, A.E. Shareef, E. Saranceva, T. Iskra, M. Dvoryatkina, E. Zhinchenko, O. Sindeeva, V. Tuchin, J. Kurths, J. Biophotonics **11**, e201700287 (2018)
20. A.N. Pavlov, A.I. Dubrovsky, A.A. Koronovskii Jr., O.N. Pavlova, O.V. Semyachkina-Glushkovskaya, J. Kurths, Chaos. Solitons Fractals **139**, 109989 (2020)
21. A.N. Pavlov, A.S. Abdurashitov, A.A. Koronovskii Jr., O.N. Pavlova, O.V. Semyachkina-Glushkovskaya, J. Kurths, Commun. Nonlin. Sci. Numer. Simulat. **85**, 105232 (2020)
22. A.N. Pavlov, A.I. Dubrovsky, A.A. Koronovskii Jr., O.N. Pavlova, O.V. Semyachkina-Glushkovskaya, J. Kurths, Chaos **30**, 073138 (2020)
23. C.-K. Peng, S.V. Buldyrev, S. Havlin, M. Simons, H.E. Stanley, A.L. Goldberger, Phys. Rev. E **49**, 1685 (1994)
24. C.-K. Peng, S. Havlin, H.E. Stanley, A.L. Goldberger, Chaos **5**, 82 (1995)
25. S.V. Buldyrev, A.L. Goldberger, S. Havlin, R.N. Mantegna, M.E. Matsa, C.-K. Peng, M. Simons, H.E. Stanley, Phys. Rev. E **51**, 5084 (1995)
26. S.G. Mallat, IEEE Trans. Pattern Anal. Mach. Intell. **11**, 674 (1989)
27. I. Daubechies, *Ten Lectures on Wavelets*. Society for Industrial and Applied Mathematics, (1992)
28. S. Thurner, M.C. Feurstein, M.C. Teich, Phys. Rev. Lett. **80**, 1544 (1998)
29. A.N. Pavlov, O.N. Pavlova, O.V. Semyachkina-Glushkovskaya, J. Kurths, Chaos **31**, 043110 (2021)
30. H.E. Stanley, L.A.N. Amaral, A.L. Goldberger, S. Havlin, P.Ch. Ivanov, C.K. Peng, Phys. A **270**, 309 (1999)
31. P. Talkner, R.O. Weber, Phys. Rev. E **62**, 150 (2000)
32. J.W. Kantelhardt, E. Koscielny-Bunde, H.H.A. Rego, S. Havlin, A. Bunde, Phys. A **295**, 441 (2001)
33. N.S. Frolov, V.V. Grubov, V.A. Maksimenko, A. Lüttjohann, V.V. Makarov, A.N. Pavlov, E. Sitnikova, A.N. Pisarchik, J. Kurths, A.E. Hramov, Sci. Rep. **9**, 7243 (2019)
34. I.M. Dremin, V.I. Furletov, O.V. Ivanov, V.A. Nechitailo, V.G. Terziev, Control Eng. Prac. **10**, 599 (2002)
35. A.N. Pavlov, A.I. Dubrovskii, O.N. Pavlova, O.V. Semyachkina-Glushkovskaya, Appl. Sci. **11**, 1182 (2021)
36. A.N. Pavlov, O.N. Pavlova, O.V. Semyachkina-Glushkovskaya, J. Kurths, Eur. Phys. J. Plus. **136**, 10 (2021)
37. O. Semyachkina-Glushkovskaya, A. Abdurashitov, A. Dubrovsky, D. Bragin, O. Bragina, N. Shushunova, G. Maslyakova, N. Navolokin, A. Bucharskaya, V. Tuchin, J. Kurths, A. Shirokov, J. Biomed. Opt. **22**, 073138 (2017)